Computer Aided Surgery, September 2008; 13(5): 243–254

informa
healthcare

BIOMEDICAL PAPER

Cardiolock: An active cardiac stabilizer. First *in vivo* experiments using a new robotized device

WAEL BACHTA[1], PIERRE RENAUD[2], EDOUARD LAROCHE[1], ANTONELLO FORGIONE[3], & JACQUES GANGLOFF[1]

[1]*LSIIT CNRS - Strasbourg I University, Ilkirch, France;* [2]*Laboratoire du Génie de la Conception (LGeCo), INSA Strasbourg, Strasbourg; and* [3]*IRCAD/EITS, University Hospital of Strasbourg, Strasbourg, France*

(Received 31 January 2008; accepted 3 June 2008)

Abstract

Off-pump Coronary Artery Bypass Grafting (CABG) is still a technically difficult procedure. The mechanical stabilizers used for local suppression of the heart excursion have been demonstrated to exhibit significant residual motion, which could lead to a lack of accuracy in performing the surgical task, particularly when using a minimally invasive surgery (MIS) approach. We therefore propose a novel active stabilizer to compensate for the residual motion whose architecture is compatible with MIS.

An experimental evaluation of a commercially available totally endoscopic stabilizer is first presented to demonstrate the unsatisfactory behavior of this device. Then, the interaction between the heart and a mechanical stabilizer is assessed *in vivo* using an animal model. Finally, the principle of active stabilization, based on the high-speed vision-based control of a piezo-actuated compliant mechanism, is presented, along with *in vivo* experimental results obtained using a prototype to demonstrate its efficiency.

Keywords: *Cardiac surgery, beating heart, minimally invasive, medical robotics, active stabilization*

Key link: http://eavr.u-strasbg.fr/wiki_en/index.php/Cardiolock

Introduction

During a conventional Coronary Artery Bypass Grafting (CABG), the heart and lungs are bypassed using an artificial heart-lung machine so that the surgeons can operate on a motionless heart. Use of the heart-lung machine has been proven to cause harmful effects in some patients, including impaired renal function, red blood cell aggregation, and neurological complications [1, 2]. Off-pump CABG has therefore been proposed as a means of preventing these deleterious effects.

The complex motion of the heart makes an off-pump CABG technically challenging. For example, the left anterior descending coronary artery may exhibit an excursion of 12.5 mm, whereas its diameter is approximately 1 mm [3] and the accuracy required for suturing is in the range of 0.1 mm. Several passive mechanical stabilizers have been proposed to overcome this difficulty by reducing the anastomosis site excursion, and these devices have been evaluated in various experimental studies. Cattin et al. [4] stabilized a coronary artery with a passive Medtronic Octopus device, assessing its performance in three pigs using a camera coupled with a laser sensor. The residual excursion in the direction perpendicular to the cardiac tissue ranged from 0.5 to 2.6 mm. Lemma et al. [3] performed a 3D heart wall motion analysis during

Correspondence: Wael Bachta, IRCAD/EITS, 1 place de l'hôpital, 67091 Strasbourg Cedex, France. Tel: +33 (0)3 88 11 91 04. Fax: +33 (0)3 88 11 91 78. E-mail: wael@eavr.u-strasbg.fr

Part of this research was previously presented at the 10th International Conference on Medical Image Computing and Computer-Assisted Intervention (MICCAI 2007) held in Brisbane, Australia, from 29 October to 2 November 2007.

ISSN 1092–9088 print/ISSN 1097–0150 online © 2008 Informa UK Ltd.
DOI: 10.1080/10929080802413129

stabilization in 10 pigs, and reported systolic-to-diastolic heart motion of more than 1.5 mm when using three different commercial passive devices. To our knowledge, very few articles have dealt with the use of a mechanical stabilizer that is compatible with the even more challenging minimally invasive off-pump CABG. Loisance et al. [5] reported the results of robot-assisted totally endoscopic CABG experiments in human subjects. One of the reported difficulties encountered by the surgeons was the significant residual motion of the passive Medtronic EndoOctopus stabilizer used in the tests, though no quantitative evaluation was provided.

Each of these groups noted the inadequate performance of commercially available stabilizers. Their experimental results are expressed in terms of residual motion, which is the end-user's point of view. However, very little information is available about the forces encountered by the stabilizer due to the heart itself. Gilhuly et al. [6] performed *in vivo* assessment of the cardiac forces in order to design a mechanical stabilizer. However, the relationship between these forces and the physiological motions, i.e., respiratory and cardiac motions, as well as the dynamics of the interaction between the stabilizer and the heart surface, were not studied in detail.

In references [7–10], several robotic systems are considered which could potentially compensate for heart motion during off-pump CABG. The principle is to synchronize a robotized tool holder with the anastomosis site movement. From a safety point of view, using a single robot to perform simultaneously both the surgical gesture and the stabilization may not be satisfactory. The robot has to undergo high accelerations to track the heart motion, and the kinetic energy of the robot poses a danger to the patient, especially when the tool is in contact with the heart surface. Moreover, the extension of this approach to MIS is not obvious. One solution consists of reducing the size of the parts that move at high speed, e.g., by using a miniature robot with endocavity mobilities, though this remains a technical challenge. An original approach was proposed by Patronik et al. [11]. In this work, a mobile robot which attaches itself to the myocardium is able to navigate on the heart surface to administer therapy.

In this paper, a novel approach is proposed which allows the separation of the stabilization and surgical tasks. We introduce the principle of an active cardiac stabilizer that allows to actively suppress the residual motion. The fundamental principle of our approach is to some extent similar to vibration cancellation techniques. Furthermore, the architecture of this new active stabilizer, called Cardiolock, is compatible with MIS.

In the next section, an experimental evaluation of a totally endoscopic Medtronic Octopus TE tissue stabilizer is provided to characterize quantitatively its adequacy with respect to off-pump CABG. Then, an experimental analysis of the interaction between the cardiac muscle and a rigid non-actuated stabilizer is presented. High-speed vision, force measurements and biological signals have been synchronously recorded during *in vivo* experiments on a pig. These data are of great interest for understanding the stabilizer behavior and improving the design of an active device. Finally, the design and principle of the active stabilizer are presented, along with the results of *in vivo* experiments using the developed prototype which show its efficiency, and the paper concludes with a discussion of further potential developments of the stabilizer.

Evaluation of a totally endoscopic stabilizer

Loisance et al. [5] pointed out the significant residual excursion of the heart when using an endoscopic stabilizer. In this section, we complete this assessment by an *in vivo* characterization of the behavior of a totally endoscopic passive stabilizer, the Medtronic Octopus TE. An experiment was carried out on a 45-kg pig which underwent full sternotomy after receiving general anesthesia. The ventilation tidal volume was set to 450 ml with a frequency of 14 breaths/minute. The recorded fundamental heart frequency was 1.08 beats/second. The heart of the animal was stabilized using the Octopus TE device. This device is attached to the operating table rail using a rigid shaft and an articulating arm (Figure 1). The latter allows ergonomic positioning in the thoracic cavity. Seven LEDs were added to the stabilizer's suction fingers as visual markers. The stabilizer configuration corresponds approximately to an entry through the subxiphoid in a human patient.

The residual displacement was measured by tracking the seven LEDs in the image of a 333-Hz high-speed camera (DALSA CAD6) with a 256×256 CCD grayscale sensor. The DeMenthon algorithm [12] was used to reconstruct the Octopus TE position and orientation. Figure 2 shows the displacement of the Octopus fingers in three directions. The peak-to-peak values are 2.2 mm, 1.6 mm and 4.2 mm in the x, y and z directions, respectively. The z direction corresponds to the anterior-posterior (AP) direction, whereas the x and y directions lie in the frontal plane. The given values are important with regard to the required surgical accuracy: they are significant compared to the 1- to 2-mm diameter of the coronary arteries. In monocular vision, the

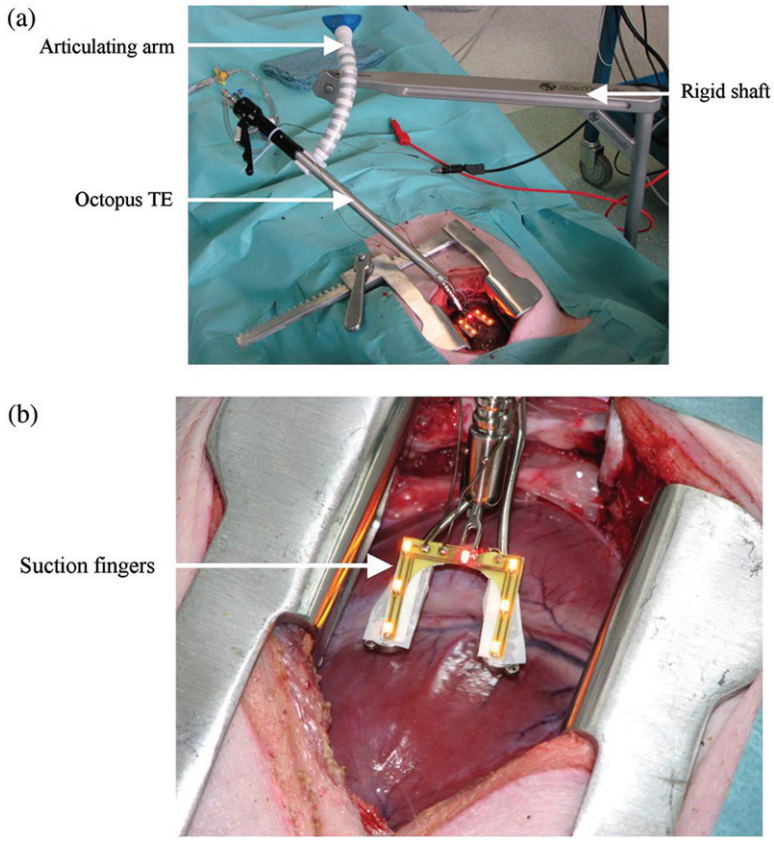

Figure 1. The experimental setup with the Octopus TE and a close-up on the distal device. [Color version available online.]

noise of 3D reconstruction is more significant with respect to the depth than the other directions. This noise is mainly projected on the z and x axes of the frame attached to the myocardium. During the evaluation, it has been noticed that the residual motion of the stabilizer suction fingers is mainly due to the displacement of the shaft.

Experimental evaluation of the heart contact forces

To complete the work presented in several previous publications focusing on heart motion analysis [13–15], we here present an experimental evaluation of the forces applied by a passively stabilized heart. This allows a better understanding of the interaction between the cardiac muscle and a mechanical stabilizer, and provides useful information for the design of a stabilizer. This custom passive stabilizer is held by a medical robot with a high mechanical stiffness, so that the residual motion should be minimized.

Experimental setup

The experiment was carried out on a 40-kg pig which underwent full sternotomy after receiving general anesthesia. The ventilation tidal volume was set to 300 ml with a frequency of 16 breaths/minute. The recorded fundamental heart frequency was 1.81 beats/second. A custom rigid stabilizer held by a medical robot was positioned on the myocardium (Figure 3). This stabilizer is composed of a stainless steel beam 10 mm in diameter and a distal device to gain access to the thoracic cavity. This distal device hosts a 6-degrees-of-freedom (6-DOF) ATI Nano-17 force sensor with a resolution of 0.0125 N for the force and 0.0625 Nmm for the torque. The stabilizer tip has been designed with a suction capability, and its residual displacement is measured using the position of a visual marker in the image of the 333-Hz high-speed camera as described above. A Navitar Precise Eye zoom lens was used to obtain a resolution of 128 pixels/mm in the experimental configuration. The ventilation was acquired through two unidirectional Honeywell Awm700 airflow sensors. The ECG signal was acquired using a 3-lead ECG cable and a Schiller Cardiovit AT-6 electrocardiograph (Figure 3). All the data acquisitions are synchronized on the camera frame-rate with software running under the Xenomai real-time operating system.

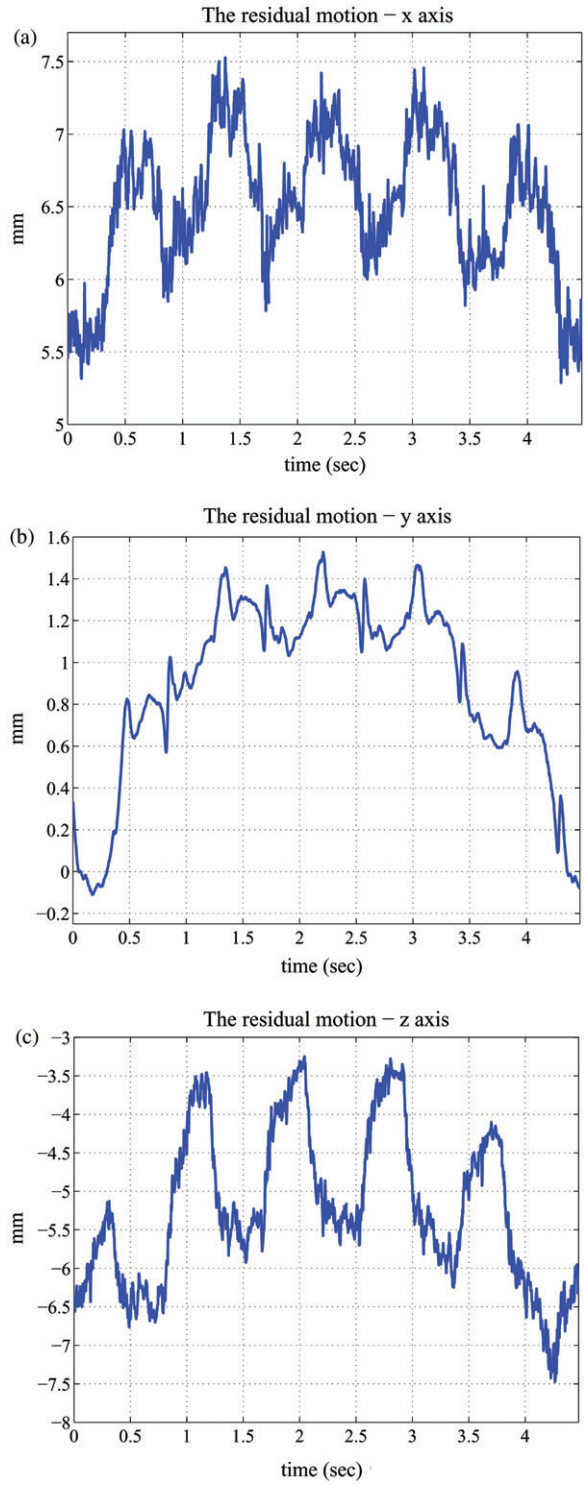

Figure 2. The residual motion of the heart during a respiratory cycle when using the Octopus TE.

Experimental results

Figure 4 shows the obtained force and torque measured during one respiratory cycle for the biological parameters given above. The corresponding peak-to-peak values are reported in Table I. The most significant force component is along the z axis, i.e., in the AP direction. The other force components are also significant, with those along the x and z axes being in a ratio of approximately 1 : 3. Torque is of small amplitude, in the region of 15 Nmm.

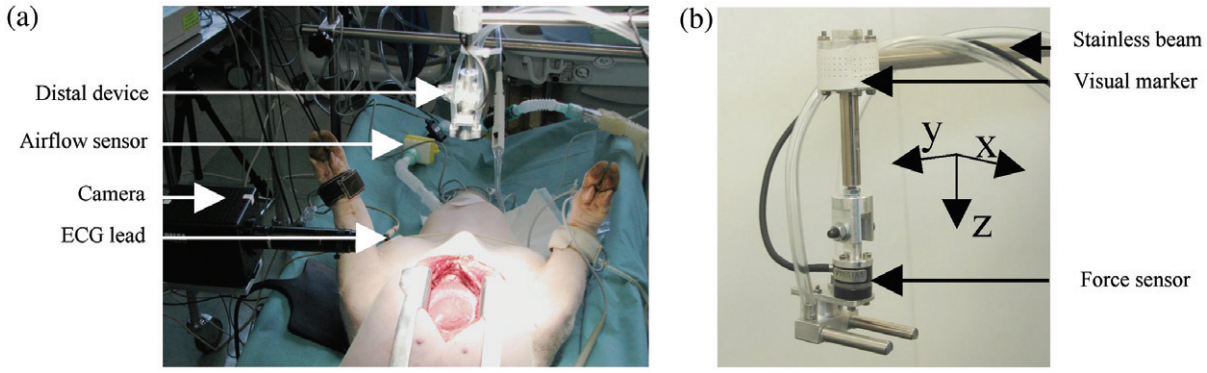

Figure 3. The experimental setup with the custom stabilizer and a close-up on the distal device. [Color version available online.]

It may be noticed that the force along the z axis contains small positive values, indicating that the heart tries to pull the stabilizer. This is due to the stabilizer's initial positioning, which is therefore important, since high positive force values could result in injuries to the myocardium. Figure 5 shows a frequency analysis of the cardiac force. Like the heart motion [14], the cardiac force is composed of two periodic components: The slow component is due to the ventilation and the faster one corresponds to the heartbeats. Note that the contribution of the ventilation harmonics is more significant along the z axis than in the other directions. Moreover, the cardiac and ventilation fundamental frequencies have the same contribution to the total force along the z axis, whereas the cardiac fundamental frequency is dominant for the other directions.

It is interesting to note in Figure 6 that the peaks of the three force components do not occur simultaneously. Furthermore, even if the amplitude of the force components in the x and y directions is lower than in the z direction, their transients are sharper. Figure 6 also shows that the force peaks are correlated with the physiological signals. Indeed, the peaks occur a short time (approximately 10 ms) after the QRS complex detection, i.e., during the systolic phase. An acquisition without ventilation shows that the cardiac movement is responsible for half of the total force along the z axis, the entire force along the y axis, and almost the entire x component (Table I). While the remaining excursion of the stabilizer tip in the presence of ventilation is approximately 0.61 mm along the z axis and 0.3 mm along the x axis, it is reduced to 0.3 mm and 0.19 mm when the ventilation is turned off (Figure 7). Even using a stiff support, the residual motion is still significant due to the bending of the stabilizer beam. The y direction corresponds to the beam axis, and the displacement due to traction is therefore negligible.

The active heart stabilizer

The active compensation principle

The required stabilization accuracy is estimated at 0.1 mm, considering the 1- to 2-mm diameter of the coronary arteries and the 0.1-mm diameter of the suturing thread. In a MIS context, the stabilizer should be a cylinder with a maximum external diameter of 10–12 mm and a length of approximately 300 mm so that the heart surface can be reached by insertion through a trocar. According to the elasticity theory, the distal stabilizer deflection due to the measured cardiac force will then exceed the required precision. The experiments with a passive stabilizer described in the previous section confirm this analysis, showing clearly the limits of passive stabilization. In fact, the displacement could be as high as 0.6 mm, which is far outside the required accuracy.

We therefore now introduce the principle of an active stabilization. Indeed, we propose an active system composed of an actuated cardiac stabilizer and an exteroceptive measurement. Using this feedback, the actuated stabilizer can be controlled so as to cancel the residual cardiac motion. Herein we use high-speed visual feedback, but any kind of exteroceptive measurement could be used.

As mentioned previously, this new principle allows the separation of the stabilization task from the surgical task. Figure 8 shows the organization of an operating room when an active stabilizing system is used. The active mechanism, which is mounted on a holder with high stiffness to achieve precise positioning in the thoracic cavity, stabilizes the area of interest with respect to the operating table. The surgical task can therefore be accomplished on a motionless operating area using a suitable surgical robot (e.g., the Da Vinci system).

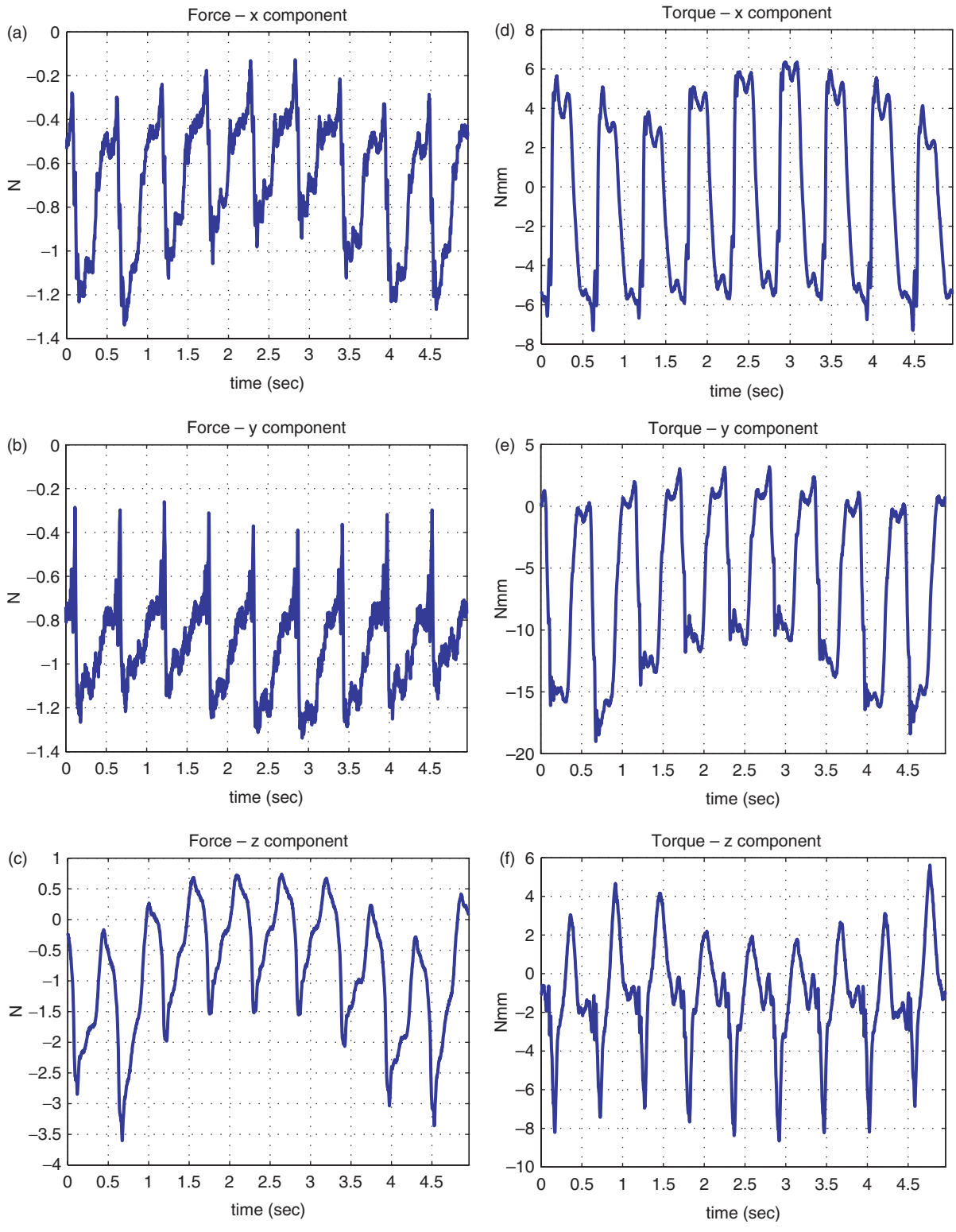

Figure 4. Measurement of the force and torque components during one respiratory cycle.

Current design

At the current stage of development, the aim of the proposed prototype (Figure 9) is to compensate for the anastomosis site displacement in the AP direction, since that is the direction in which the maximum force and residual motion are encountered. Globally, the proposed device consists of two parts. The first active part is composed of a 1-DOF

Table I. Peak-to-peak force and torque values.

	F_x (N)	F_y (N)	F_z (N)	T_x (Nmm)	T_y (Nmm)	T_z (Nmm)
With ventilation	1.2	1.0	3.8	13	20	13
Without ventilation	0.8	1.0	2.0	12	12	10

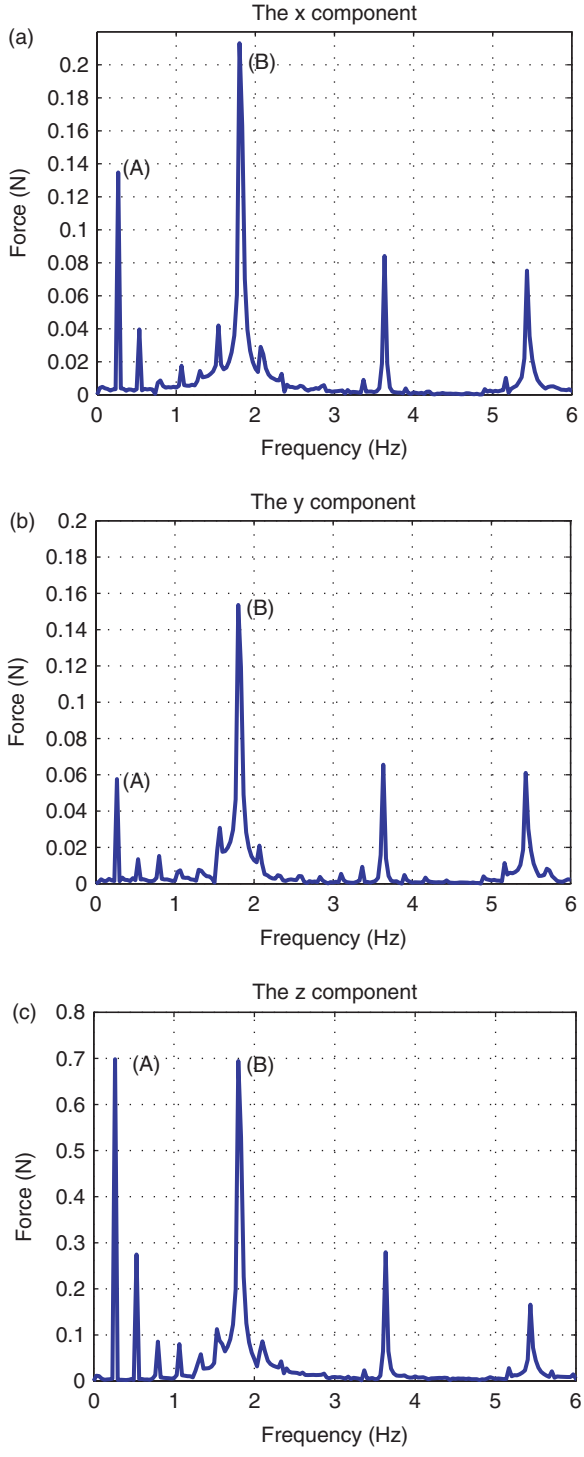

Figure 5. Spectral analysis of the heart force. (A) and (B) are the peaks corresponding to the respiratory and cardiac fundamental frequencies, respectively.

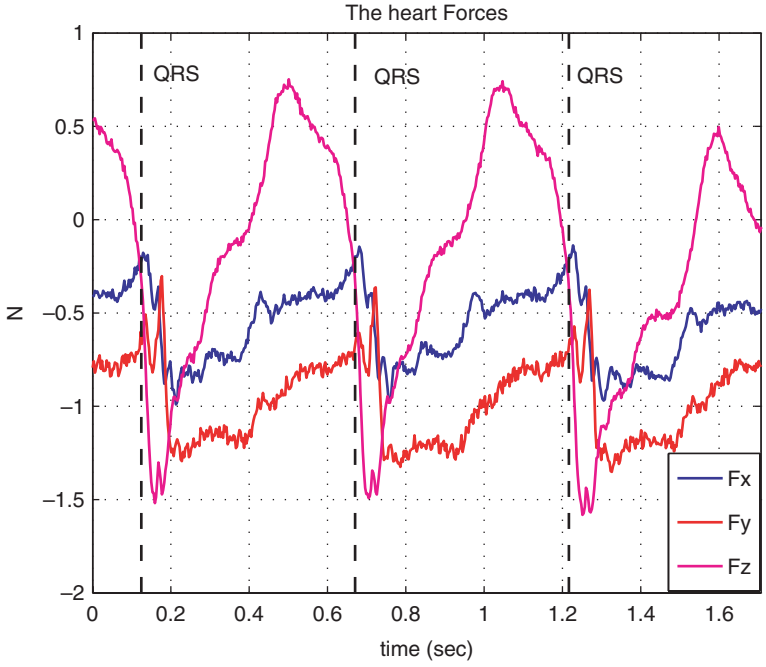

Figure 6. Correlation of the heart contact force with the ECG signal. [Color version available online.]

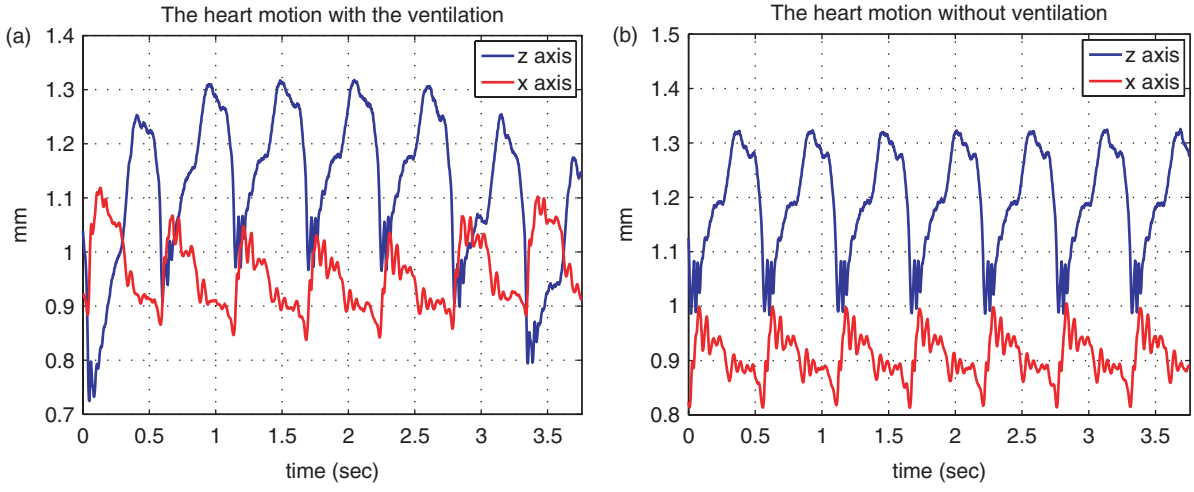

Figure 7. The heart residual motion with and without ventilation. [Color version available online.]

closed-loop mechanism which remains outside the patient's body in a MIS context. The other part is a beam 10 mm in diameter and 300 mm in length. This component, whose dimensions are compatible with MIS, can be simply locked onto the first part. Figure 9 shows that the closed-loop mechanism is composed of a piezo actuator (Cedrat Technologies) and three revolute compliant joints. Piezo actuation is adopted to obtain high dynamics, and compliant joints are used to avoid backlash. The closed-loop mechanism is designed like a compliant slider crank mechanism, in order to transform the piezo actuator translation into a rotation of the beam, as described in Figure 10. In this figure, for description purposes only, the compensation is then decomposed in two sequential steps: in the upper part one can see a magnified deflection due to an external load, and in the lower part the cancellation of the tip displacement by modifying the geometry of the closed-loop mechanism. The mechanism dimensions are chosen with respect to geometric, force equilibrium and fatigue constraints. Further details on the design methodology are given in reference [16].

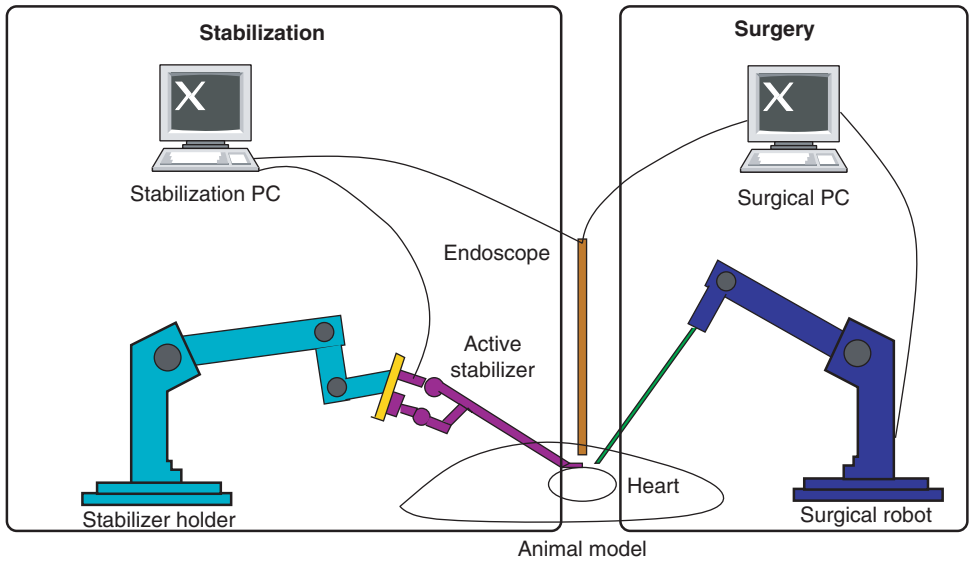

Figure 8. The organization of the operating room when an active stabilizer is used. [Color version available online.]

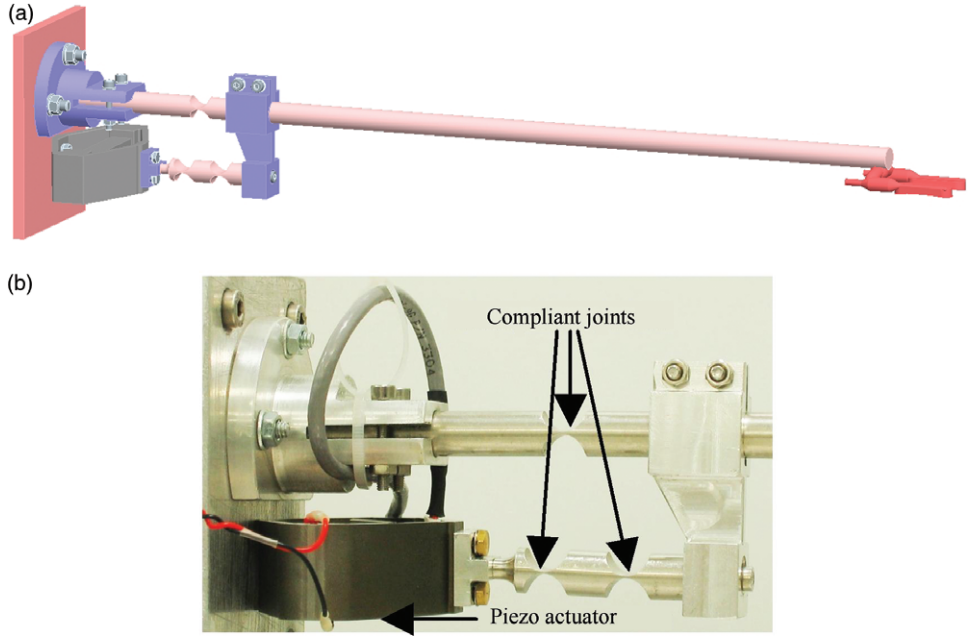

Figure 9. (a) The current prototype of the active stabilizer – a CAD global view. (b) Detail of the closed-loop mechanism on the current prototype. [Color version available online.]

In a MIS context, asepsy can be obtained by separating the device into two parts: the first, external, subsystem can be wrapped in a sterile bag and the other, internal, part can be sterilized using an autoclave. To be fully compatible with MIS, a distal end needs to be designed to provide more degrees of freedom for the placement on the myocardium. Finally, the Cardiolock is held by a mechanism which allows handling of the trocar constraint either passively or actively (e.g., via a Remote Center of Motion mechanism).

High-speed visual servoing

Figure 11 is a block diagram detailing the relationship between the control signal u and the visual measurement v. $\mathbf{G}(s)$ and $\mathbf{P}(s)$ are two transfer functions respectively relating the piezo actuator displacement α and the cardiac force f to the stabilizer tip position y. The computed control signal u is converted into an analog voltage with a digital-to-analog conversion modeled by a Zero Order Holder (ZOH). This voltage corresponds to

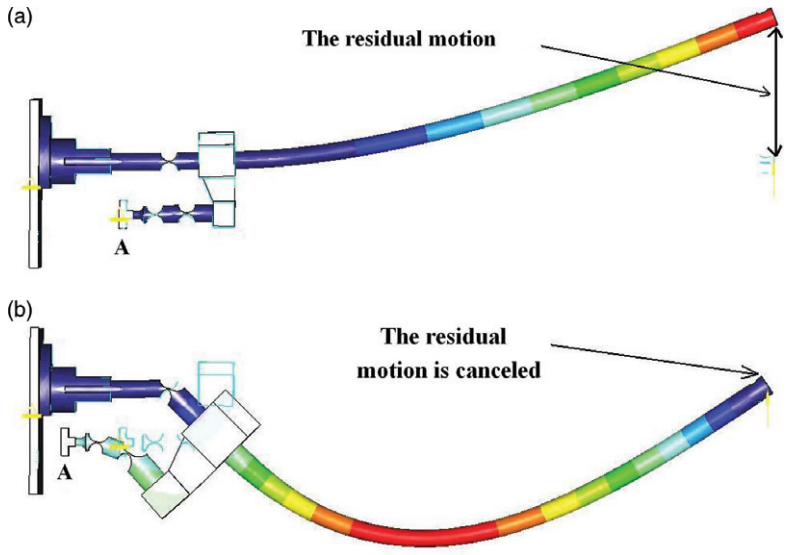

Figure 10. A finite element analysis of the compensation. The actuator controls the horizontal position of point A. Displacements are magnified for the sake of clarity. [Color version available online.]

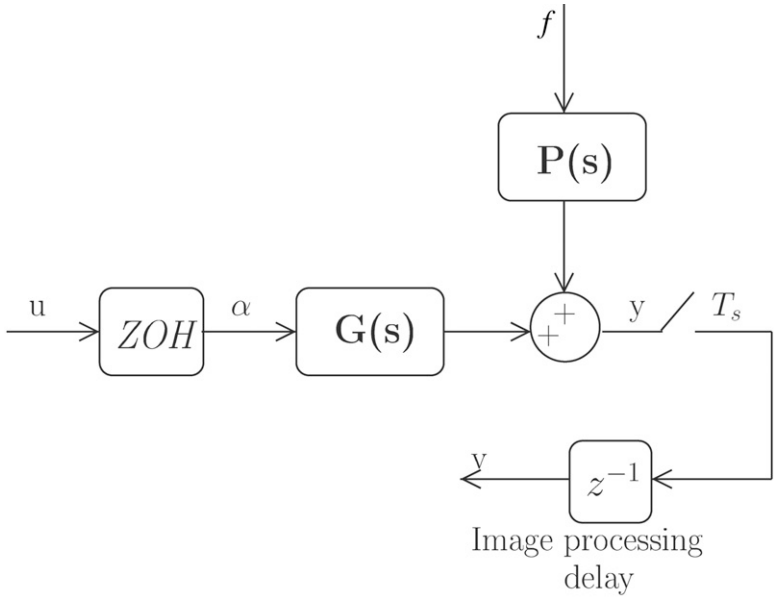

Figure 11. Modeling of the system.

the required displacement of the piezo actuator, obtained via the high dynamics of the piezo local control loop. The output y is measured using the position of a visual marker v in the image given by a high-speed camera with a sampling period $T_s = 3$ ms. A time-delay of one period is required for the acquisition and processing of the current image. The transfer function **G** has been identified using classical techniques [17], while **P** is constructed by approximation from the poles of **G** and an experimentally estimated static gain [16]. Using the visual information v, the control signal u is computed by means of an H_∞ feedback controller [18] tuned to fulfill two objectives. The first objective is to reject with high performances the cardiac force effect in order to achieve a good stabilization of the area of interest. The second objective is to make the control loop immune with respect to modeling uncertainties, since the model used does not take into account the cardiac tissue mechanical properties.

Initial in vivo *results*

The experimental setup described in the previous section was used to carry out *in vivo* active

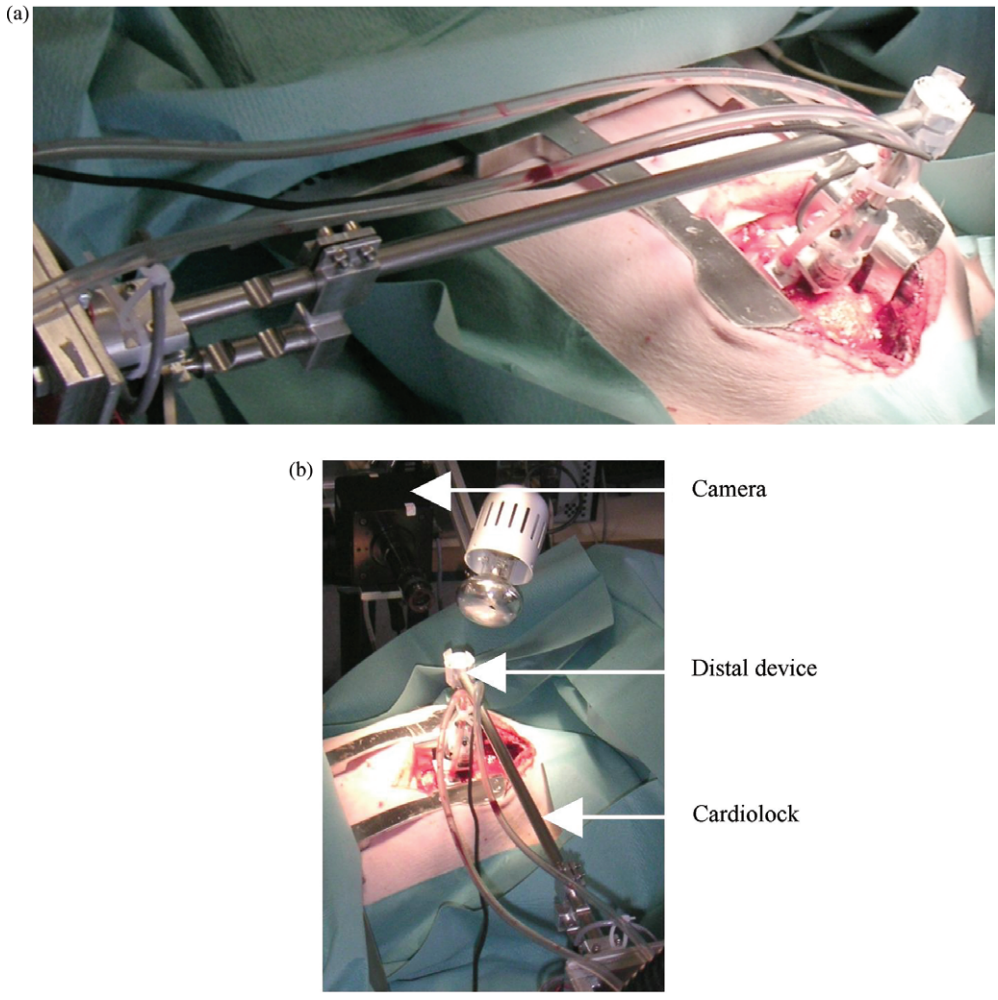

Figure 12. The Cardiolock device during an experimental validation. [Color version available online.]

stabilization experiments (Figure 12). The beam of the passive stabilizer was simply replaced by the novel actuated mechanism. The same distal device is used to provide easy access to the thoracic cavity. Figure 13 reports the results of two stabilization tests. In both cases, the controller was switched on 6 seconds after the beginning of the experiment. The peak-to-peak heart excursion was then divided by four. The RMS of the residual motion in the anterior-posterior direction is 0.37 mm before activation of the active stabilization, which corresponds to the deflection measured in the earlier section entitled *Experimental evaluation of the heart contact forces*, and 0.03 mm after activation. Since the frequency of the respiratory motion is low, it is completely suppressed, whereas the cardiac component is partially filtered. In the second experiment, the force along the z axis was recorded (Figure 13). Only a slight variation of the force is observed. This may be explained by the small displacement, approximately 0.3 mm, imposed at the local area of interest to achieve the stabilization. Since the cardiac force during active stabilization is almost equivalent to the force when using passive stabilization, the use of active stabilization should not cause any deleterious effect on the myocardium.

Conclusion

In this paper, *in vivo* experiments have been conducted to demonstrate the efficiency of an active stabilizer for CABG in a MIS approach. In an initial study, significant residual motion was demonstrated in a commercial device. The interaction between the heart and a custom mechanical stabilizer was then assessed *in vivo*. The principle of active stabilization has been introduced and the design and control of a 1-DOF prototype has been described. Initial *in vivo* experimental results using the current prototype are promising. Future work will include the design of enhanced control laws to improve the current behavior of Cardiolock. The development of a multi-DOF mechanism with the

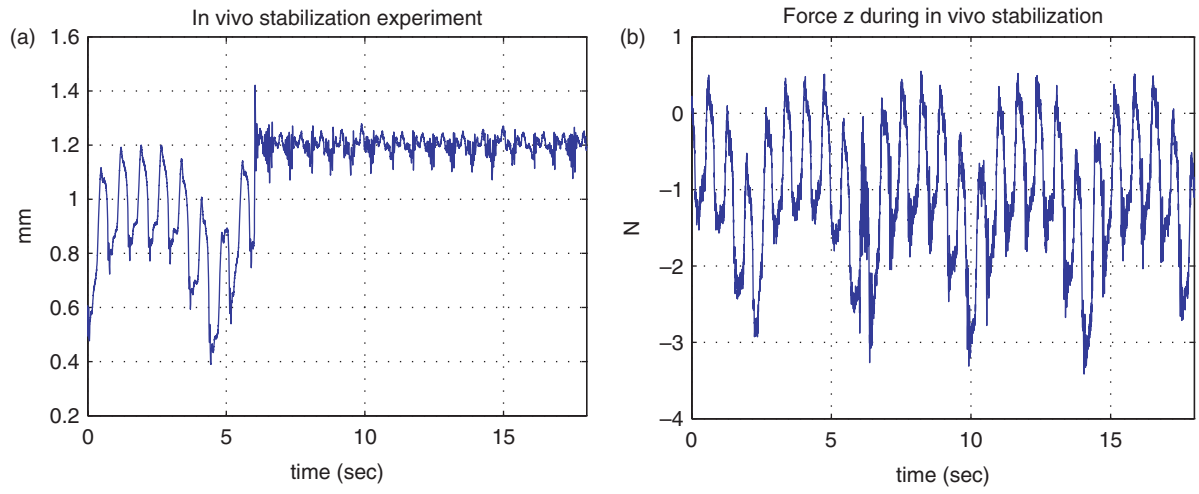

Figure 13. *In vivo* stabilization results. (a) Measured motion. (b) Recorded contact force. The active stabilization starts after 6 seconds.

appropriate vision measurement will also be investigated in order to compensate for all possible residual motions.

***Declaration of interest*:** The authors report no conflicts of interest. The authors alone are responsible for the content and writing of the paper.

References

1. Roach G, Kanchuger M, Mangano C. Adverse cerebral outcomes after coronary bypass surgery. New England J Medicine 1996;335:1857–1863.
2. Laffey J, Boylan J, Cheng D. The systemic inflammatory response to cardiac surgery: Implications for the anesthesiologist. Anesthesiology 2002;97:215–252.
3. Lemma M, Mangini A, Redaelli A, Acocella F. Do cardiac stabilizers really stabilize? Experimental quantitative analysis of mechanical stabilization. Interact Cardiovasc Thorac Surg 2005;4(3):222–226.
4. Cattin P, Dave H, Grunenfelder J, Székely G, Turina M, Zund G. Trajectory of coronary motion and its significance in robotic motion cancellation. Eur J Cardiothorac Surg 2004;25:786–790.
5. Loisance D, Nakashima K, Kirsch M. Computer-assisted coronary surgery: Lessons from an initial experience. Interact Cardiovasc Thorac Surg 2005;4:398–401.
6. Gilhuly T, Salcudean S, Ashe K, Lichtenstein S, Lawrence P. Stabilizer and surgical arm design for cardiac surgery. In: Proceedings of the IEEE International Conference on Robotics and Automation (ICRA-98), Leuven, Belgium, May 1998. pp 699–704.
7. Thakral A, Wallace J, Tolmin D, Seth N, Thakor N. Surgical Motion Adaptive Robotic Technology (S.M.A.R.T.): Taking the motion out of physiological motion. In: Niessen WJ, Viergever MA, editors. Proceedings of the Fourth International Conference on Medical Image Computing and Computer-Assisted Intervention (MICCAI 2001), Utrecht, The Netherlands, October 2001. Lecture Notes in Computer Science 2208. Berlin: Springer; 2001. pp 317–325.
8. Nakamura Y, Kishi K, Kawakami H. Heartbeat synchronization for robotic cardiac surgery. In: Proceedings of the IEEE International Conference on Robotics and Automation (ICRA 2001), Seoul, Korea, May 2001. pp 2014–2019.
9. Ginhoux R, Gangloff J, de Mathelin M, Soler L, Sanchez M, Marescaux J. Active filtering of physiological motion in robotized surgery using predictive control. IEEE Trans Robotics 2005;21(1):67–79.
10. Bebek O, Cavusoglu M. Intelligent control algorithms for robotic-assisted beating heart surgery. IEEE Trans Robotics 2007;23(3):468–480.
11. Patronik N, Zenati M, Riviere C. Preliminary evaluation of a mobile robotic device for navigation and intervention on the beating heart. Comput Aided Surg 2005;10(5): 225–232.
12. Oberkampf D, DeMenthon D, Davis L. Iterative pose estimation using coplanar feature points. CVGIP: Image Understanding 1996;63(3):495–511.
13. Cuvillon L, Gangloff J, de Mathelin M, Forgione A. Toward robotized beating heart TECABG: Assessment of the heart dynamics using high-speed vision. In: Duncan JS, Gerig G, editors. Proceedings of the 8th International Conference on Medical Image Computing and Computer-Assisted Intervention (MICCAI 2005), Palm Springs, CA, October 2005. Part II. Lecture Notes in Computer Science 3750. Berlin: Springer; 2005. pp 551-558.
14. Ortmaier T, Gröger M, Boehm D, Falk V, Hirzinger G. Motion estimation in beating heart surgery. IEEE Trans Biomed Eng 2005;52(10):1729–1740.
15. Shechter G, Resar J, McVeigh E. Displacement and velocity of the coronary arteries: Cardiac and respiratory motion. IEEE Trans Med Imag 2006;25(3):369–375.
16. Bachta W, Renaud P, Laroche E, Forgione A, Gangloff J. Design and control of a new active cardiac stabilizer. In: Proceedings of the IEEE/RSJ International Conference on Intelligent Robots and Systems (IROS 2007), San Diego, CA, 29 October-2 November 2007.
17. Ljung L. System identification: Theory for the user, 2nd ed. Upper Saddle River, NJ: Prentice-Hall; 1999.
18. Doyle J, Glover K, Khargonekar P, Francis B. State-space solutions to standard H_2 and H_∞ control problems. IEEE Trans Automatic Control 1989;34(8):831–847.